Pergamon

Int. J. Solids Structures Vol. 35, No. 36, pp. 5159–5171, 1998

Printed in Great Britain
0020-7683/98/$—see front matter

PII: S0020-7683(97)00252-7

THE HYBRID CRACK-TIP ELEMENT APPROACH TO THERMO-ELASTIC CRACKS

C. N. DUONG† and J. YU
McDonnell Douglas Corporation, Now, The Boeing Company, Mail Code C078-0209, 2401 E. Wardlow Road, Long Beach CA 90807-5309, U.S.A.

(*Received* 10 *December* 1996; *in revised form* 15 *August* 1997)

Abstract—The stress intensity factors for a thermal crack problem are computed directly from the crack tip singular field as it was embedded in a specialized crack-tip element. The method gives accurate results without modeling a very refined mesh near the crack tip and without evaluating additional line and/or area integrals for the "modified" path independent integrals as suggested by most current methods for thermoelastic cracks. © 1998 Elsevier Science Ltd. All rights reserved.

1. INTRODUCTION

Airframe structures in High Speed Civil Transport (HSCT) are exposed to elevated temperatures during their service life due to aerodynamic heating (see e.g. Bray and Starke, 1992). As a result, these structures are subjected to thermally induced stresses which in turn may reduce their residual strength and their fatigue life. This is in contrast to conventional aircraft fatigue analysis in which thermal stresses can be neglected due to the small thermal variations.

Fatigue and fracture related predictions are normally based on a single or a few near tip parameters, depending on the crack model employed. However, the stress intensity factors (for small scale yielding) and the J-integral (for large scale yielding) in any circumstances are recognized as the most vital parameters for these predictions (see e.g. Paris *et al.*, 1961; Swedlow, 1965; Begley and Landes, 1972). Accurate estimates for fatigue life and residual strength of structural components, therefore, require an accurate method to compute these characterized fracture parameters. While the current methods for evaluating K_I and K_{II} of a thermoelastic crack are claimed to be accurate and mostly by way of finite elements, they are neither efficient nor simple (see e.g. Wilson and Yu, 1979; Kishimoto *et al.*, 1980; Shih *et al.*, 1986; Kuo and Riccardella, 1987). The first approach of these methods is to reformulate a thermal stress crack problem in terms of a crack surface loading problem by using the principle of linear superposition (see e.g. Wilson and Yu, 1979). The crack surface loads must be determined from thermal stresses of an uncracked geometry under the prescribed temperature field. It is obvious that this approach is not efficient since one has to solve two separate (uncracked and cracked) problems. Further, the analysis for a crack surface loading problem usually employs a finer mesh than that for a stress free crack problem to enable to model the prescribed surface loads accurately. In the second approach to the thermoelastic crack analysis, a (new) modified definition for J is proposed since the original Rice J-integral is no longer path independent nor appropriate for thermal cracks (see e.g. Wilson and Yu, 1979; Kishimoto *et al.*, 1980; Shih *et al.*, 1986; Kuo and Riccardella, 1987). These modified J either contain an additional area integral term beside the usual line integral term (Wilson and Yu, 1979; Kishimoto *et al.*, 1980) or are expressed completely in terms of an area integral (Shih *et al.*, 1986). Since these methods involve an area integration over an arbitrary domain enclosing the crack tip, they require necessarily a highly accurate stress solution near the crack tip. These methods, therefore, degrade the merit of the J-integral approach on taking advantage of the path independent property of

† Author to whom correspondence should be addressed. Tel.: 001 562 593 1421. Fax: 001 562 982 7367. E-mail: c322189@hi5003.mdc.com.

J which can be calculated based on solutions far away from the singular crack tip. To eliminate the undesired area integration, Kuo and Riccardella (1987) suggested a new modified J which involves only a path independent line integral. However, this definition for J contains either a free expansion displacement field or a conjugate temperature field which are the solutions of another (second) boundary-value problem. This method is, therefore, also not efficient. In addition, other methods for computing energy release rates and the stress intensity factors for elastostatic problem under general loading conditions which include the body force have been proposed recently (see e.g. Raju and Shivakumar, 1990; Lee and Grosse, 1993, 1995). Since these latter methods include body forces, they can also be applied to the thermo-elastic crack problems. However, the methods still require evaluation of an area integral enclosing the crack tip when the prescribed body force is not uniformly distributed.

The objective of this paper is to present an alternate method for evaluating K_{I} and K_{II}, which gives accurate and efficient results without performing the cumbersome line and/or area integrations. This is possible because the crack tip singular behavior[1] is embedded in a specialized crack tip element so that the crack tip region is accurately modeled and the stress intensity factors (together with the nodal displacements) are determined directly from the finite element analysis. The crack tip element is formulated based on hybrid assumed stress approach first proposed by Pian (1964) and, Pian and Tong (1969) three decades ago. This hybrid approach for linearly elastic crack was considered by Luk (1972). Even though there is a potential application of the approach to other cracked problems such as fully plastic and thermoelastic cracks, to our knowledge no one to date has considered such applications. The evaluation of the J-integral for large scale yielding by a plastic crack tip element has been addressed recently by the authors (Duong and Yu, 1996). Both theoretical development as well as the numerical implementation for the approach are detailed there. The reader who is unfamiliar with the hybrid crack tip element approach should refer to that reference. The present work is the result of our current research at MDC on thermal-mechanical fatigue crack growth. In the initial phase of the study, we limit our investigation to the thermoelastic crack, and as the study progresses we would eventually include thermo-plastic and visco-plastic cracks.

2. BASIC EQUATIONS OF THERMOELASTICITY

Within the framework of the uncoupled quasi static thermoelasticity theory, the governing equations for a 2-D domain without body force are (see e.g. Fung, 1965):

$$\sigma_{ij,j} = 0 \tag{2.1}$$

$$\varepsilon_{ij} = 1/2(u_{i,j} + u_{j,i}) \tag{2.2}$$

$$\sigma_{ij} = \lambda \varepsilon_{kk}\delta_{ij} + 2G\varepsilon_{ij} - \beta\Gamma\delta_{ij}, \tag{2.3}$$

with the following boundary conditions

$$T_i = \bar{T}_i \quad \text{on } S_\sigma, \tag{2.4}$$

$$u_i = \bar{u}_i \quad \text{on } S_u, \tag{2.5}$$

where σ_{ij}, ε_{ij} and u_i are the stress tensor, strain tensor and displacement vector, respectively; λ and G are the Lamé constant and shear modulus; Γ is the relative temperature measured from some reference stress free temperature; T_i is the traction vector; $\beta = [\alpha E/(1-\nu^*)]$ with E being the Young modulus, α being the thermal coefficient of linear expansion, $\nu^* = \nu$,.

[1] The asymptotic stress field for a thermoelastic crack had shown to be the same as that for a linearly elastic crack (Sih, 1962). This, of course, can also be seen from the linear supposition of a surface loading crack problem with the uncracked thermal stress problem as mentioned earlier for a thermal crack problem.

the Poisson ratio, for plane stress and $\nu^* = 2\nu$ for plane strain. The temperature field Γ is determined separately from heat conduction analysis, and by assumption it is a prescribed field for the present thermoelastic problem.

As is well known, the thermoelastic problem without body force can be reformulated in terms of an "isothermal" problem with a prescribed ("thermally") body force by using Duhamel–Newmann Analogy (see e.g. Fung, 1965). The stress solution of the problem stated above (Problem I) can be expressed as

$$\sigma_{ij}^{(\mathrm{I})} = \sigma_{ij}^{(\mathrm{II})} - \beta\Gamma\delta_{ij}, \tag{2.6}$$

where $\sigma_{ij}^{(\mathrm{II})}$ is the stress tensor of the following (isothermal) boundary value problem (Problem II):

$$\sigma_{ij,j}^{(\mathrm{II})} + F_i = 0 \tag{2.7}$$

$$\varepsilon_{ij} = 1/2(u_{i,j} + u_{j,i}) \tag{2.8}$$

$$\sigma_{ij} = \lambda\varepsilon_{kk}\delta_{ij} + 2G\varepsilon_{ij} \tag{2.9}$$

$$F_i = \beta\Gamma_{,i} \tag{2.10}$$

subjected to

$$T_i^{(\mathrm{II})} = \bar{T}_i + \beta\Gamma n_i \quad \text{on } S_\sigma \tag{2.11}$$

$$u_i = \bar{u}_i \quad \text{on } S_u. \tag{2.12}$$

As mentioned earlier, since Γ is a prescribed temperature field, $\sigma_{ij}^{(\mathrm{I})}$ is determined once $\sigma_{ij}^{(\mathrm{II})}$ of the equivalently isothermal problem is solved. Moreover, since Γ is usually prescribed as a smooth function, $\beta\Gamma\delta_{ij}$ contains no singularity and the stress intensity factors of Problem I are the same as those of Problem II.[2] It should be emphasized that since Problem II is a standard, isothermal, linearly elastic boundary value problem with the body force given by $\beta\Gamma_{,i}$, the hybrid assumed stress approach can be applied directly to such problem without any necessary modification for the governing variational principle employed by the approach. For that reason, all developments below are for solving Problem II. For simplicity, we drop the superscript (II) (to designate Problem II) in all notions for stresses and traction in the next Subsections.

3. FINITE ELEMENT FORMULATION

An efficient way to solve the crack problem is to divide the domain into two subdomains (see Fig. 1): the crack tip region (subdomain A) and the domain outside of the crack tip region (subdomain B); each is formulated by a different finite element approach. The crack tip region is modeled by the hybrid elements which contain the crack tip singular behavior. On the other hand, the outside of the crack tip region is modelled by the regular (displacement-based) elements. This mixed element type modeling is preferred over the same (one) element type approach because the near tip behavior can be modeled accurately by the hybrid elements while the far field region is adequately and cost efficiently represented by the regular elements which do not require matrix inversion in their stiffness formation as in that for the hybrid elements (see Section 3.2). This mixed modelling (for a problem with a "thermally" body force) is compatible because one can pose Problem II alternately

[2] In design practice, the heat transfer problem is normally solved separately first for the temperature distribution inside the structure. This analysis is carried out under the assumption of no crack inside the structure, and it is followed by a thermo-elastic fracture analysis. Thus, the effect of the crack on the thermal flow has been ignored in the present analysis.

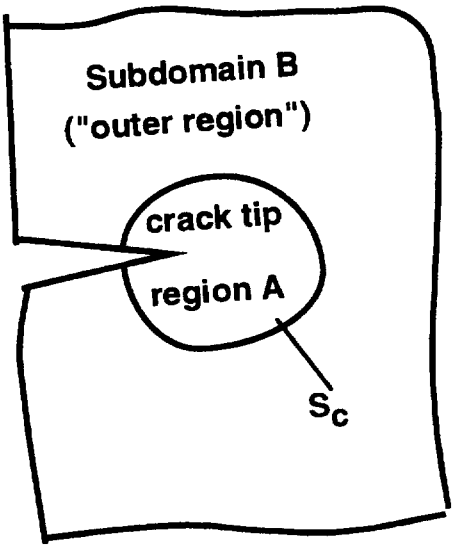

Fig. 1. Subdomains A and B of the Problem II (with "thermal" body force). S_c is the common boundary.

as: find stress and strain fields on each subdomain A and B which satisfy eqns (2.7)–(2.10) with the following boundary conditions:

For subdomain A,

$$T_i = \bar{T}_i + \beta\Gamma n_i \quad \text{on } S_\sigma \tag{3.1}$$

$$T_i = Q_i' + \beta\Gamma n_i \quad \text{on } S_c \tag{3.2}$$

$$u_i = \bar{u}_i \quad \text{on } S_u \tag{3.3}$$

For subdomain B,

$$T_i = \bar{T}_i + \beta\Gamma n_i \quad \text{on } S_\sigma \tag{3.4}$$

$$T_i = -Q_i' - \beta\Gamma n_i \quad \text{on } S_c \tag{3.5}$$

$$u_i = \bar{u}_i \quad \text{on } S_u, \tag{3.6}$$

where S_c is the common boundary of the two subdomains and $Q_i' + \beta\Gamma n_i$ is the (unknown) traction acting on S_c with Q_i' being part of that traction vector,[3] these two subproblems clearly can be solved independently by a different finite element approach providing that Q_i' is known. However, since Q_i' is unknown, one has to solve these two subproblems simultaneously with the following compatibility condition:

$$u_i^{(A)} = u_i^{(B)} \quad \text{along } S_c. \tag{3.7}$$

Since both assumed displacement and hybrid assumed stress approaches interpolate the displacement on the element boundaries from the nodal displacements (see next sections), condition (3.7) is identically satisfied as long as the discretized subdomains A and B have the common nodes along S_c. Further, as demonstrated in the next two Subsections, the element force vector associated with the unknown traction Q_i' on S_c for regular elements

[3] We express the unknown traction as $Q_i' + \beta\Gamma n_i$ so that it is similar to the conditions given on S_σ [see equation (2.11)].

bordering S_c is the same but opposite in sign with that for the neighboring hybrid elements of the crack tip region on the other side of S_c. Thus, the element force vectors associated with Q_i' will cancel out with each other when the two subproblems are solved together (simultaneously) with their domain having the common nodes along S_c, so that no explicit expression for Q_i' is required. The above procedure is clearly equivalent to mixed element type approach which deliberately uses different element types based on different finite element formulation for different regions of the structure without formulating in terms of two separate subproblems. Nevertheless, the above procedure is able not only to show the compatibility of the mixed modeling approach rigorously but also to help us in retaining or eliminating certain matrices from hybrid formulation consistently. The finite element formulation for each subdomain is given in the next two sections.

3.1. *Finite element formulation for the outer region*

The outside of the crack tip region is modeled by the regular (displacement-based) elements. The finite element equations are derived based on the principle of virtual displacement.

$$\int_V \sigma_{ij}\delta\varepsilon_{ij}\,\mathrm{d}V - \int_V \beta\Gamma_{,i}\delta u_i\,\mathrm{d}V + \int_{S_c}(Q_i' + \beta\Gamma n_i)\delta u_i\,\mathrm{d}S + \int_{S_\sigma}(\bar{T}_i + \beta\Gamma n_i)\delta u_i\,\mathrm{d}S = 0. \tag{3.8}$$

Rewrite $\beta\Gamma_{,i}\,\delta u_i$ of the second integral above as $(\beta\Gamma\delta u_i)_{,i} - \beta\Gamma\delta u_{i,i}$, and apply divergence theorem for $\int_V (\beta\Gamma\delta u_i)_{,i}\,\mathrm{d}V$ results in

$$\int_V \sigma_{ij}\delta\varepsilon_{ij}\,\mathrm{d}V + \int_V \sigma_{ij}^{(t)}\delta\varepsilon_{ij}\,\mathrm{d}V + \int_{S_c} Q_i'\delta u_i\,\mathrm{d}S + \int_{S_\sigma}\bar{T}_i\delta u_i\,\mathrm{d}S, \tag{3.9}$$

$$\sigma_{ij}^{(t)} = \beta\Gamma\delta_{ij}; \tag{3.10}$$

δ_{ij} is the Kronecker delta; the relations $\beta\Gamma\delta u_{i,i} = \beta\Gamma\delta u_{i,j}\delta_{ij} = \sigma_{ij}^{(t)}\delta\varepsilon_{ij}$ and $\delta u_i = 0$ on S_u have been used in the derivation. Dividing the analyzed domain into n elements, assuming the displacement field in each element to be a smooth function of its nodal displacements and carrying out the minimization process with respect to the nodal displacement lead to the following finite element equations

$$\sum^{n}(\underset{\sim}{K}^{(e)}\underset{\sim}{q}^{(e)}) = \sum^{n}(\underset{\sim}{F}^{(e)} + \underset{\sim}{F}_t^{(e)} + \underset{\sim}{F}_{Q'}^{(e)}). \tag{3.11}$$

$\underset{\sim}{K}^{(e)}$ and $\underset{\sim}{F}^{(e)}$ are the usual element stiffness matrix and the usual (mechanical) element force vector. $\underset{\sim}{F}_{Q'}^{(e)}$ is the element force vector associated with traction Q_i' acting on S_c; it will be cancelled out during the structure assemblage by a same vector but opposite in sign from the neighboring hybrid elements but on the other side of S_c as demonstrated later in the next Subsection. $\underset{\sim}{F}_t^{(e)}$ in the above equation is given by $\int_{V_n}\underset{\sim}{B}^T\underset{\sim}{\sigma}^{(t)}\,\mathrm{d}V$ where $\underset{\sim}{B}$ is the strain–displacement matrix. Thus, for the present problem (with thermally body force), one must include $\underset{\sim}{F}_t^{(e)}$ in addition to the usual stiffness matrix term and the usual (mechanical) load vector.

3.2. *Finite element formulation for the crack tip region*

The crack tip region is modeled by the hybrid elements. The variation principle which governs the assumed stress hybrid model is given as

$$\Pi_H = \sum^{n}\left(\int_{V_n} B(\sigma_{ij})\,\mathrm{d}V - \int_{\partial V_n} T_i u_i\,\mathrm{d}S + \int_{S_{\sigma_n}}\bar{T}_i u_i\,\mathrm{d}S\right), \tag{3.12}$$

where:

$B(\sigma_{ij})$ = complementary elastic strain energy density $C_{ijkl}\,\sigma_{ij}\,\sigma_{kl}$;
σ_{ij} = stress tensor;
n = number of singular subelements associated with crack tip region;
u_i = displacement components along boundaries;
T_i = surface traction components;
$\bar{T}_i$ = prescribed surface traction components over S_{σ_n};
V_n = volume of subelement n;
∂V_n = entire boundary of V_n;
S_{σ_n} = surface of V_n over which the surface traction T_i are prescribed.

In this formulation, the assumed stress tensor σ_{ij} must satisfy the nonhomogeneous equilibrium equations

$$\sigma_{ij,j}+\beta\Gamma_{,i}=0. \tag{3.13}$$

The assumed stress tensor is expressed as a sum of a function which satisfies the homogeneous equilibrium equation and the particular solution $\beta\Gamma\delta_{ij}$. Because the asymptotic stress near the crack tip is known, the homogeneous part of the assumed function for σ_{ij} in each subelement can be divided into two parts: one-part contains the regular stress expression $\underset{\sim}{P}\underset{\sim}{\beta}$ and the other contains the special terms with proper stress singularity $\underset{\sim}{P}_s\underset{\sim}{\beta}_s$, i.e.,

$$\underset{\sim}{\sigma}=\underset{\sim}{P}\underset{\sim}{\beta}+\underset{\sim}{P}_s\underset{\sim}{\beta}_s+\underset{\sim}{\sigma}_t, \tag{3.14}$$

where $\underset{\sim}{P}\underset{\sim}{\beta}$ is generally a polynomial in spatial coordinates, which satisfies the equilibrium equations; $\underset{\sim}{P}_s\underset{\sim}{\beta}s$ contains the Williams asymptotic stress terms (Williams, 1957); $\underset{\sim}{\sigma}_t$ is the known particular solution $\beta\Gamma\delta_{ij}$. The coefficient $\underset{\sim}{\beta}$ is independent from subelement to subelement while $\underset{\sim}{\beta}_s$ represents the intensity of singularity and is common to all subelements in the crack tip element region. The surface tractions for each subelement are related to the assumed stress distribution by $\underset{\sim}{T}=\underset{\sim}{\nu}\underset{\sim}{\sigma}$ and can be expressed as

$$\underset{\sim}{T}=\underset{\sim}{R}\underset{\sim}{\beta}+\underset{\sim}{R}_s\underset{\sim}{\beta}_s+\underset{\sim}{R}_t. \tag{3.15}$$

The boundary displacements $\underset{\sim}{u}$ of a subelement are interpolated in terms of its nodal displacement $\underset{\sim}{q}$, i.e.,

$$\underset{\sim}{u}=\underset{\sim}{L}\underset{\sim}{q}. \tag{3.16}$$

Substituting (3.14)–(3.16) into (3.12) and enforcing the stationary conditions of the functional Π_H with respect to the variations of $\underset{\sim}{\beta}$, $\underset{\sim}{\beta}_s$, and $\underset{\sim}{q}$ yield an "independent" equation

$$\underset{\sim}{H}\underset{\sim}{\beta}+\underset{\sim}{H}_s\underset{\sim}{\beta}_s+\underset{\sim}{H}_t-\underset{\sim}{G}\underset{\sim}{q}=0 \tag{3.17}$$

for each subelement since $\underset{\sim}{\beta}$ is independent from subelement to subelement, and the following (coupled) system of equations for all subelements in the crack tip region

$$\sum^{n}(\underset{\sim}{k}\underset{\sim}{q}+\underset{\sim}{m}^T\underset{\sim}{\beta}_s)=\sum^{n}\underset{\sim}{F}_1 \tag{3.18}$$

$$\sum^{n}(\underset{\sim}{m}\underset{\sim}{q}+\underset{\sim}{n}\underset{\sim}{\beta}_s)=\sum^{n}\underset{\sim}{F}_2 \tag{3.19}$$

where

$$\underline{k} = \underline{G}^T \underline{H}^{-1} \underline{G} \quad \text{(stiffness matrix of a single subelement)} \tag{3.20}$$

$$\underline{m} = \underline{G}_s - \underline{H}_s^T \underline{H}^{-1} \underline{G} \tag{3.21}$$

$$\underline{n} = \underline{H}_s^T \underline{H}^{-1} \underline{H}_s - \underline{H}_{ss} \tag{3.22}$$

$$\underline{F}_1 = \bar{\underline{Q}} + \underline{F}_{Q'} + \underline{F}_t + \underline{G}^T \underline{H}^{-1} \underline{H}_t^T - \underline{G}_t^T. \tag{3.23}$$

$$\underline{F}_2 = \underline{H}_{st}^T - \underline{H}_s^T \underline{H}^{-1} \underline{H}_t^T. \tag{3.24}$$

$$\bar{\underline{Q}} = \int_{S_{\sigma_n}} \bar{\underline{T}}^T \underline{L} \, \mathrm{d}S \tag{3.25}$$

$$\underline{F}_{Q'} = -\int_{S_c} \underline{Q}' \underline{L} \, \mathrm{d}S \tag{3.26}$$

$$\underline{F}_t = \int_{S_c + S_{\sigma_n}} \underline{\sigma}_t \underline{L} \, \mathrm{d}S \tag{3.27}$$

$$\underline{H} = \int_{V_n} \underline{P}^T \underline{C} \underline{P} \, \mathrm{d}V \tag{3.28}$$

$$\underline{H}_s = \int_{V_n} \underline{P}^T \underline{C} \underline{P}_s \, \mathrm{d}V \tag{3.29}$$

$$\underline{H}_{ss} = \int_{V_n} \underline{P}_s^T \underline{C} \underline{P}_s \, \mathrm{d}V \tag{3.30}$$

$$\underline{H}_t = \int_{V_n} \underline{\sigma}_t^T \underline{C} \underline{P} \, \mathrm{d}V \tag{3.31}$$

$$\underline{H}_{st} = \int_{V_n} \underline{\sigma}_t^T \underline{C} \underline{P}_s \, \mathrm{d}V \tag{3.32}$$

$$\underline{G} = \int_{\partial V_n} \underline{R}^T \underline{L} \, \mathrm{d}S \tag{3.33}$$

$$\underline{G}_s = \int_{\partial V_n} \underline{R}_s^T \underline{L} \, \mathrm{d}S \tag{3.34}$$

$$\underline{G}_t = \int_{\partial V_n} \underline{R}_t^T \underline{L} \, \mathrm{d}S. \tag{3.35}$$

Table 1(a). Stress matrices for a rectangular hybrid element. (Subelement type 1 in Fig. 2)

(1) $\underline{\sigma} = \{\sigma_x, \sigma_y, \tau_{xy}\} = \underline{P}\{\beta_1, \beta_2, \beta_3, \ldots, \beta_{18}\} + K_p \underline{P}_s$

where $\underline{P}$ is as follows:

$$\begin{bmatrix} 1 & y & 0 & 0 & 0 & x & 0 & y^2 & 0 & x^2 & xy & 0 & xy^2 & y^3 & 0 & x^2y & x^3/3 & 0 \\ 0 & 0 & 1 & x & 0 & 0 & y & 0 & x^2 & y^2 & 0 & xy & 0 & 0 & x^3 & y^3/3 & xy^2 & x^2y \\ 0 & 0 & 0 & 0 & 1 & -y & -x & 0 & 0 & -2xy & -y^2/2 & -x^2/2 & -y^3/3 & 0 & 0 & -xy^2 & -x^2y & -x^3/3 \end{bmatrix}$$

and $\underline{P}_s$ is given by

$$\begin{bmatrix} \frac{1}{\sqrt{2r}}\cos\frac{\theta}{2}\left[1-\sin\frac{\theta}{2}\sin\frac{3\theta}{2}\right] & -\frac{1}{\sqrt{2r}}\sin\frac{\theta}{2}\left[2+\cos\frac{\theta}{2}\cos\frac{3\theta}{2}\right] \\ \frac{1}{\sqrt{2r}}\cos\frac{\theta}{2}\left[1+\sin\frac{\theta}{2}\sin\frac{3\theta}{2}\right] & \frac{1}{\sqrt{2r}}\sin\frac{\theta}{2}\cos\frac{\theta}{2}\cos\frac{3\theta}{2} \\ \frac{1}{\sqrt{2r}}\cos\frac{\theta}{2}\sin\frac{\theta}{2}\cos\frac{3\theta}{2} & \frac{1}{\sqrt{2r}}\cos\frac{\theta}{2}\left[1-\sin\frac{\theta}{2}\sin\frac{3\theta}{2}\right] \end{bmatrix}$$

(2) $\underline{T} = \{-\tau_{xyAB}, -\sigma_{yAB}, \tau_{xyCD}, \sigma_{yCD}, \sigma_{xBD}, \tau_{xyBD}, \sigma_{xAC}, \tau_{xyAC}\} = \underline{R}\{\beta_1, \beta_2, \ldots, \beta_{18}\} + K_p \underline{R}_s$

where $\underline{R}$ is as follows

$$\begin{bmatrix} 0 & 0 & 0 & 0 & -1 & 0 & x & 0 & 0 & 0 & 0 & x^2/2 & 0 & 0 & 0 & 0 & 0 & x^3/3 \\ 0 & 0 & -1 & -x & 0 & 0 & 0 & 0 & -x^2 & 0 & 0 & 0 & 0 & 0 & x^3/3 & 0 & 0 & 0 \\ 0 & 0 & 0 & 0 & 1 & -b & -x & 0 & 0 & -2bx & -b^2/2 & -x^2/2 & -b^3/3 & 0 & 0 & -b^2x & -bx^2 & -x^3/3 \\ 0 & 0 & 1 & x & 0 & 0 & b & 0 & x^2 & b^2 & 0 & bx & 0 & 0 & x^3 & b^3/3 & b^2x & bx^2 \\ 1 & y & 0 & 0 & 0 & a & 0 & y^2 & 0 & a^2 & ay & 0 & ay^2 & y^3 & 0 & a^2y & a^3/3 & 0 \\ 0 & 0 & 0 & 0 & 1 & -y & -a & 0 & 0 & -2ay & -y^2/2 & -a^2/2 & -y^3/3 & 0 & 0 & -ay^2 & -a^2y & -a^3/3 \\ -1 & -y & 0 & 0 & 0 & 0 & 0 & -y^2 & 0 & 0 & 0 & 0 & 0 & -y^3 & 0 & 0 & 0 & 0 \\ 0 & 0 & 0 & 0 & -1 & y & 0 & 0 & 0 & 0 & y^2/2 & 0 & -y^3/3 & 0 & 0 & 0 & 0 & 0 \end{bmatrix}$$

and $\underline{R}_s$ is evaluated from the singular stress term ($\underline{P}_s$) along the boundary of the element but is omitted from here due to lack of its representation in a simple form.

Table 1(b). Boundary displacement matrix for a four-node rectangular hybrid element. (Subelement type 1 in Fig. 2)

$\underline{u} = \{u_{AB}, v_{AB}, u_{CD}, v_{CD}, u_{BD}, v_{BD}, u_{AC}, v_{AC}\} = \underline{L}\{q_1, q_2, \ldots, q_8\}$

where $\underline{L}$ is given by

$$\begin{bmatrix} (1-s^{1/2}) & 0 & s^{1/2} & 0 & 0 & 0 & 0 & 0 \\ 0 & (1-s^{1/2}) & 0 & s^{1/2} & 0 & 0 & 0 & 0 \\ 0 & 0 & 0 & 0 & s & 0 & (1-s) & 0 \\ 0 & 0 & 0 & 0 & 0 & s & 0 & (1-s) \\ 0 & 0 & (1-t) & 0 & t & 0 & 0 & 0 \\ 0 & 0 & 0 & (1-t) & 0 & t & 0 & 0 \\ (1-t^{1/2}) & 0 & 0 & 0 & 0 & 0 & t^{1/2} & 0 \\ 0 & (1-t^{1/2}) & 0 & 0 & 0 & 0 & 0 & t^{1/2} \end{bmatrix}$$

$\underline{C}$ is the elastic compliance matrix; typical matrices for $\underline{P}$, $\underline{P}_s$, $\underline{R}$, $\underline{R}_s$ and $\underline{L}$ are given in Tables 1 and 2 as discussed in details at the end of this Subsection. Since $\underline{F}_I$ cancels out with $\underline{G}_I^T$ during the assemblage phase, these matrices are not computed for each element and they can be omitted from the definition for $\underline{F}_1$. Further, since the two subdomains (the crack tip region and the outside of the crack tip region) have common nodes along S_c, it is

Table 2(a). Stress matrices for a rectangular hybrid element. (Subelement type 1 in Fig. 2)

(1) $\underset{\sim}{\sigma} = \{\sigma_x, \sigma_y, \tau_{xy}\} = \underset{\sim}{P}\{\beta_1, \beta_2, \beta_3, \ldots, \beta_{10}\} + K_p \underset{\sim}{P}_s$

where $\underset{\sim}{P}$ is as follows:

$$\begin{bmatrix} 1 & y & x & y^2 & x^2 & xy & xy^2 & y^3 & x^2y & x^3/3 \\ 0 & 0 & 0 & 0 & y^2 & 0 & 0 & 0 & y^3/3 & xy^2 \\ 0 & 0 & -y & 0 & -2xy & -y^2/2 & -y^3/3 & 0 & -xy^2 & -x^2y \end{bmatrix}$$

(2) $\underset{\sim}{T} = \{-\tau_{xyAB}, -\sigma_{yAB}, \tau_{xyCD}, \sigma_{yCD}, \sigma_{xBD}, \tau_{xyBD}, \sigma_{xAC}, \tau_{xyAC}\} = \underset{\sim}{R}\{\beta_1, \beta_2, \ldots, \beta_{10}\} + K_p \underset{\sim}{R}_s$

where $\underset{\sim}{R}$ is as follows

$$\begin{bmatrix} 0 & 0 & 0 & 0 & 0 & 0 & 0 & 0 & 0 & 0 \\ 0 & 0 & 0 & 0 & 0 & 0 & 0 & 0 & 0 & 0 \\ 0 & 0 & -b & 0 & -2bx & -b^2/2 & -b^3/3 & 0 & -b^2x & -bx^2 \\ 0 & 0 & 0 & 0 & b^2 & 0 & 0 & 0 & b^3/3 & b^2/x \\ 1 & y & a & y^2 & a^2 & ay & ay^2 & y^3 & a^2y & a^3/3 \\ 0 & 0 & -y & 0 & -2ay & -y^2/2 & -y^3/3 & 0 & -ay^2 & -a^2y \\ -1 & -y & 0 & -y^2 & 0 & 0 & -y^3 & 0 & 0 & 0 \\ 0 & 0 & y & 0 & 0 & y^2/2 & y^3/3 & 0 & 0 & 0 \end{bmatrix}$$

Table 2(b). Boundary displacement matrix for a four-node rectangular hybrid element. (Subelement type 2 in Fig. 2)

$\underset{\sim}{u} = \{u_{AB}, v_{AB}, u_{CD}, v_{CD}, u_{BD}, v_{BD}, u_{AC}, v_{AC}\} = \underset{\sim}{L}\{q_1, q_2, \ldots, q_8\}$

where $\underset{\sim}{L}$ is given by

$$\begin{bmatrix} (1-s)^{1/2} & 0 & 1-(1-s)^{1/2} & 0 & 0 & 0 & 0 & 0 \\ 0 & (1-s)^{1/2} & 0 & 1-(1-s)^{1/2} & 0 & 0 & 0 & 0 \\ 0 & 0 & 0 & 0 & s & 0 & (1-s) & 0 \\ 0 & 0 & 0 & 0 & 0 & s & 0 & (1-s) \\ 0 & 0 & (1-t^{1/2}) & 0 & t^{1/2} & 0 & 0 & 0 \\ 0 & 0 & 0 & (1-t^{1/2}) & 0 & t^{1/2} & 0 & 0 \\ (1-t) & 0 & 0 & 0 & 0 & 0 & t & 0 \\ 0 & (1-t) & 0 & 0 & 0 & 0 & 0 & t \end{bmatrix}$$

clear that $\underset{\sim}{F}_{Q'}$ of the hybrid elements bordering to S_c will cancel out with those from neighboring regular elements on the other side of S_c.

It should be emphasized that only eqns (3.18) and (3.19), not (3.16), will enter the global (structure) equations since eqn (3.16) is independent from subelement to subelement and is determined after solving for the unknown $\underset{\sim}{\beta}_s$ and the nodal displacements. Rewriting (3.19) as

$$\underset{\sim}{\beta}_s = -\underset{\sim}{N}^{-1}\underset{\sim}{M}\underset{\sim}{q}^* + \underset{\sim}{N}^{-1}\underset{\sim}{F}_2^* \tag{3.36}$$

and substituting (3.36) into (3.18) for $\underset{\sim}{\beta}_s$ results in

$$\underset{\sim}{K}_c\underset{\sim}{q}^* = \underset{\sim}{F}_1^* - \underset{\sim}{M}\underset{\sim}{N}^{-1}\underset{\sim}{F}_2^*, \tag{3.37}$$

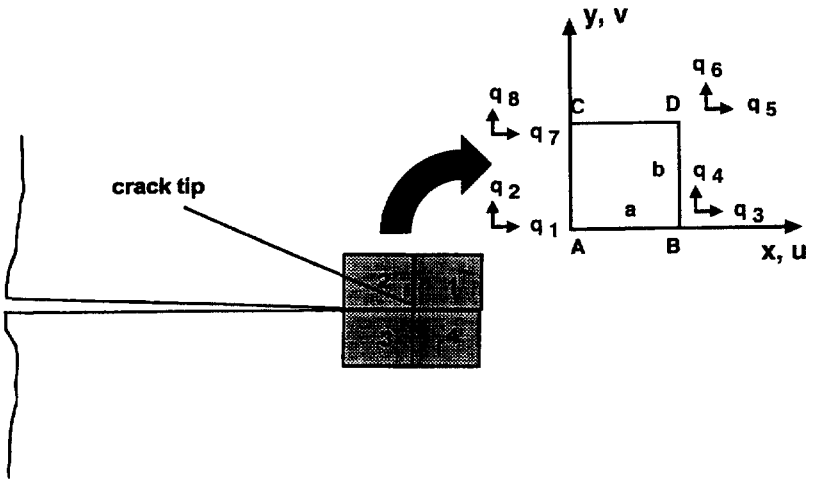

Fig. 2. Crack tip element with subelements. The local coordinates and degrees of freedom for a subelement are also shown.

where

$$\underset{\sim}{K}_c = \underset{\sim}{K} - \underset{\sim}{M}^T \underset{\sim}{N}^{-1} \underset{\sim}{M}. \tag{3.38}$$

$\underset{\sim}{M}$, $\underset{\sim}{N}$, $\underset{\sim}{K}$, $\underset{\sim}{q}^*$, $\underset{\sim}{F}_1^*$ and $\underset{\sim}{F}_2^*$ are the assemblages of $\underset{\sim}{m}$, $\underset{\sim}{n}$, $\underset{\sim}{k}$, $\underset{\sim}{q}$, $\underset{\sim}{F}_1$ and $\underset{\sim}{F}_2$, respectively, over N subelements of the elastic crack tip element; $\underset{\sim}{K}_c$ is the crack tip element stiffness matrix. Equation (3.37) is the force–displacement matrix relation for the crack tip element and it can be assembled into the global equations for the whole structure in the usual manner.

In the present analysis, the crack tip element consists of four squared subelements formulated by (3.12) as shown in Fig. 2. The matrices $\underset{\sim}{P}$, $\underset{\sim}{R}$, and $\underset{\sim}{L}$ for subelement type 1 are listed in Tables 1(a) and (b). The corresponding matrices for subelement type 2 are in Tables 2(a) and (b). The assumed stress fields satisfy identically the equilibrium equations. Further, the assumed stress field in subelement type 2 also fulfills the traction free condition on the crack surfaces. All four subelements have the common $\underset{\sim}{P}_s$ and $\underset{\sim}{\beta}_s$ where $\underset{\sim}{\beta}_s$ are mode I and mode II stress intensity factors and $\underset{\sim}{P}_s$ corresponds to the angular functions of the first two terms of Williams asymptotic series (Williams, 1957).

4. NUMERICAL EXAMPLES

To illustrate the use of the hybrid crack tip element and to examine the accuracy of the method, two example problems are solved. The first one involves an edge cracked strip being subjected to a linear temperature variation across its width as shown in Fig. 3. The temperature equals T_0 at $x = W/2$ and decreases linearly to $-T_0$ at $x = -W/2$. This problem had been analyzed by Wilson and Yu (1979) and Shih *et al.* (1986). Due to symmetry, only upper half of the strip is modeled. Different meshes are used for evaluating the normalized stress intensity factor $K_I/[\sqrt{\pi a}\alpha E T_0/(1-\nu)]$, and the results are summarized in Table 3. In all analyses, a half crack tip element is used and all regular elements are four-node isoparametric. From the table, the difference in the normalized K_I between the meshes of 204 and 551 nodes is only 1.6%. The normalized K_I based on the mesh of 204 nodes is found to be less than 9% from the average result obtained by Wilson and Yu (1979) with a mesh of 147 nodes and less than 5% from that obtained by Shih *et al.* (1986) with a mesh of 273 nodes. Based on this single example, the present method seems to be little more efficient than the domain integration method proposed by Shih *et al.* and less efficient than Wilson and Yu's method. The latter comparison should not be overlooked since all elements in Wilson and Yu's analysis are eight-node elements and thus more expensive. Their result is reported to be 3% higher than the convergent solution.

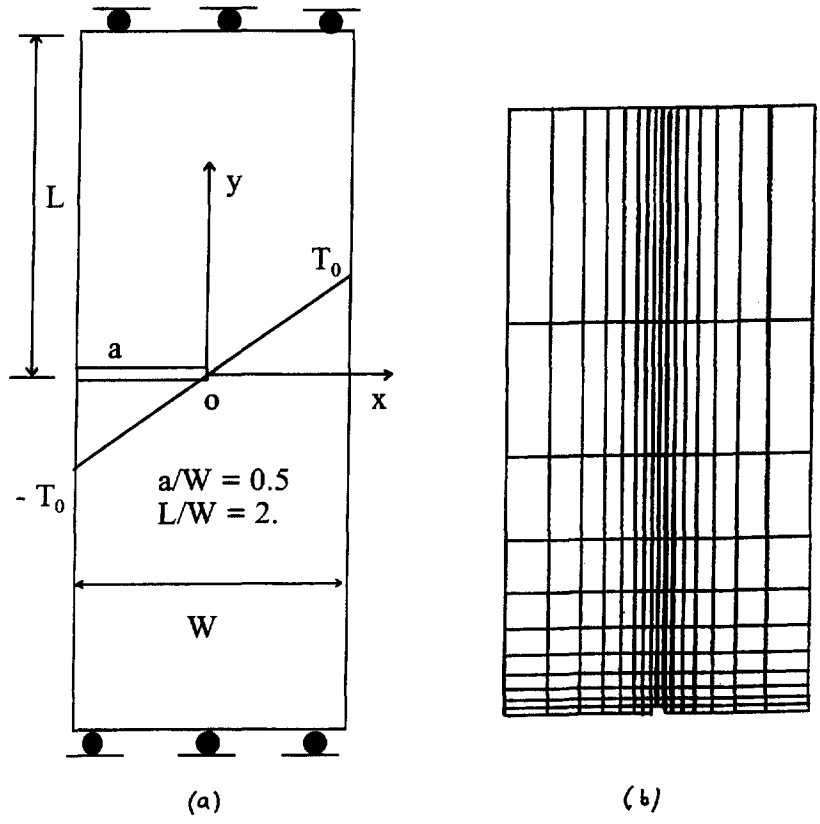

Fig. 3. An edge cracked strip under linear temperature distribution across its width. (a) Geometry. (b) Finite element mesh of the upper half model.

Table 3. Mesh sensitivities study of the crack tip element approach for Wilson and Yu problem

Number of nodes	Normalized K_I
204	0.4638
255	0.4654
300	0.471
551	0.4715

The second problem will be used to compare the present method with the design sensitivity approach (Lee and Grosse, 1993, 1995). Since all problems considered in these references are not thermo-elastic, for simplicity, we had selected the problem of an edge cracked plate under gravity as the second test case (see Fig. 4). The material properties of the plate are $E = 10{,}000$ psi, $v = 0.3$ and the gravity force is 1 lb/in^3. The problem is nonsymmetric because of the loading condition. With the aid of Duhamel–Newmann Analogy (see e.g. Fung, 1965), this problem had been solved equivalently within the present context of thermo-elasticity as an edge cracked plate under a temperature field $Y(x, y) = -0.1y$ with one end fixed while the other end is subjected to a uniform stress of 80 psi. Based on the mesh of 103 nodes, K_I, K_{II} and J are found to be 75.1 psi $\sqrt{\text{in}}$, 10.5 psi $\sqrt{\text{in}}$ and 0.576 psi-in, respectively. The present result for J is about 3% of that obtained by Lee and Grosse (1993) with a mesh of 113 nodes and with eight-node isoparametric elements.

Through the results of the two test cases, we would like to make the following two remarks. First, the computing efficiency of the present method is possibly the same as those

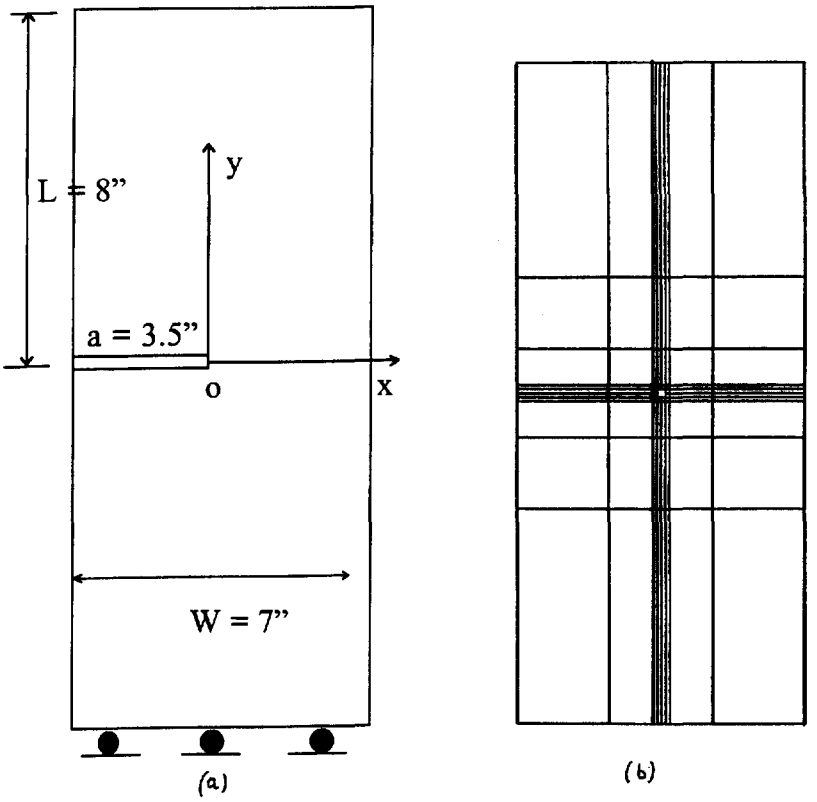

Fig. 4. An edge cracked plate under gravity. (a) Geometry. (b) Finite element mesh.

of the existing methods for problems with simple geometries and loading conditions. Second, since the intensity factors K_I and K_{II} are obtained directly from the finite element analysis as part of its solution, the advantage of the method becomes obvious for mixed mode problem when an extra step must be taken in decomposing the modified J or the energy release rate into K_I and K_{II}.

5. CONCLUSION

An alternate method for evaluating the stress intensity factors of a thermal crack problem has been proposed. This method employs a specialized crack tip element, which gives efficient and accurate results. The crack tip element is compatible with the displacement-based elements so that it can be implemented in most commercial finite element codes. Since no additionally special data is required beside the usual finite element model and since a relatively coarser mesh in many cases can be used in the analysis, the method is quite attractive from the user's standpoint.

After this work was completed, we learned from one of the reviewers that Benzley (1974) and Emery *et al.* (1975, 1977) had developed similar crack tip elements but based on the assumed displacement approach. Since these singular elements are incompatible with the isoparametric elements, special transition elements must be used along with the crack tip element. We would like to acknowledge their work.

REFERENCES

Begley, J. A. and Landes, J. D. (1972) The J integral as a fracture criterion. *ASTM STP* **514**, 1–20.
Benzley, S. E. (1974) Representation of singularities with isoparametric finite elements. *International Journal For Numerical Methods in Engineering* **8**, 537–545.

Bray, G. H. and Starke, E. A. (1992) The effect of elevated temperature exposure on fatigue crack growth retardation. *Scripta Metallurgica et Materialia* **23,** 3055–3066.

Duong, C. N. and Yu, J. (1996) On the evaluation of the *J*-integral by a plastic crack tip element. *International Journal of Fracture* **81,** 1–25.

Emery, A. F., Cupps, F. J. and Neighbors, P. K. (1975) The use of singularity programming in finite element calculations of elastic stress intensity factors, plane and axisymmetric-applied to thermal stress fracture. *ASME Computational Fracture Mechanics*, pp. 35–48.

Emery, A. F., Neighbors, P. K., Kobayashi, A. S. and Love, W. J. (1977) Stress intensity factors in edge cracked plates subjected to transient thermal singularities. *ASME Journal of Pressure Vessel Technology* **99,** 100–105.

Fung, Y. C. (1965) *Foundations of Solid Mechanics*. Prentice-Hall, Englewood Cliffs, NJ.

Kishimoto, K., Aoki, S. and Sakata, M. (1980) On the path-independent integral-*J*. *Engineering Fracture Mechanics* **13,** 841–850.

Kuo, A. and Riccardella, P. C. (1987) Path-independent line integrals for steady-state, two-dimensional thermoelasticity. *International Journal of Fracture* **35,** 71–79.

Lee, T. W. and Grosse, I. R. (1993) Energy release rate by a shape design sensitivity approach. *Engineering Fracture Mechanics* **44,** 807–819.

Lee, T. W. and Grosse, I. R. (1995) A shape design sensitivity approach for two-dimensional mixed-mode fracture analysis under general loading. *Journal of Applied Mechanics* **62,** 952–958.

Luk, C. H. (1972) Assumed stress hybrid element method for fracture mechanics and elastic–plastic analysis. Technical Report AFOSR TR73-0493.

Paris, P. C., Gomez, M. P. and Anderson, M. E. (1961) A rational analytic theory of fatigue. *The Trend in Engineering* **13,** 9–14.

Pian, T. H. H. (1964) Derivation of element stiffness matrices by assumed stress distribution. *AIAA Journal* **2,** 1333–1336.

Pian, T. H. H. and Tong, P. (1969) Basis of finite element methods for solid continua. *International Journal of Numerical Methods in Engineering* **1,** 3–28.

Raju, I. S. and Shivakumar, K. N. (1990) An equivalent domain integral method in the two-dimensional analysis of mixed mode crack problems. *Engineering Fracture Mechanics* **37,** 707–725.

Shih, C. F., Moran, B. and Nakamura, T. (1986) Energy release rate along a three-dimensional crack front in a thermally stressed body. *International Journal of Fracture* **30,** 79–102.

Sih, G. C. (1962) On the singular character of thermal stress near a crack tip. *Journal of Applied Mechanics* **29,** 587–589.

Swedlow, J. L. (1965) On Griffith's theory of fracture. *International Journal of Fracture* **1,** 210–216.

Williams, M. L. (1957) On the stress distribution at the base of a stationary crack. *Journal of Applied Mechanics* **24,** 109–114.

Wilson, W. K. and Yu, I. W. (1979) The use of the *J*-integral in thermal stress crack problems. *International Journal of Fracture* **15,** 377–387.